SAND2020-1426C
Proceedings of the 2020 28th Conference on Nuclear Engineering
Joint With the ASME 2020 Power Conference
ICONE28-POWER2020
August 2-6, 2020, Anaheim, California, USA

ICONE28-POWER2020-16409

MELCOR MODELING OF COMBINED ACCIDENT TOLERANT FUEL AND REACTOR CORE ISOLATION COOLING SYSTEM OPERATION

Chris Faucett[1], Bradley Beeny
Sandia National Laboratories
Albuquerque, NM

Karen Vierow Kirkland
Texas A&M University
College Station, TX

ABSTRACT

The work presented in this paper presents new techniques for modeling the combined use of the Reactor Core Isolation Cooling (RCIC) System and Accident Tolerant Fuel (ATF) in a Boiling Water Reactor (BWR). With guidance from Sandia National Laboratories' Severe Accident Analysis department, a MELCOR BWR model was developed from open source literature. The demonstration shown herein simulates BWR long-term station blackout (LTSBO) conditions with the Nuclear Regulatory Commission's (NRC) MELCOR severe accident analysis code. By combining state-of-the-art MELCOR modeling practices with new, physics-based RCIC System and ATF MELCOR inputs, this BWR model provides a contemporary platform for BWR severe accident simulations.

The authors are investigating the combined use of the RCIC System and ATF as a means of passively enhancing reactor safety. The benefits of this approach were evaluated by performing simulations using traditional fuel designs (i.e. Zircaloy cladding) and ATF with an iron-chromium-aluminum (FeCrAl) clad under BWR LTSBO conditions. ATF performance was evaluated using severe accident metrics, specifically event sequence timings and the hydrogen production rate from cladding oxidation. Preliminary results show delayed core degradation timelines with less hydrogen production for ATF simulations. Although the results are limited in scope, the presented analysis could easily be expanded to a full-scale uncertainty study that considers a range of severe accident boundary conditions.

This paper describes objective technical results and analysis. Any subjective views or opinions that might be expressed in the paper do not necessarily represent the views of the U.S. Department of Energy or the United States Government.

Keywords: MELCOR, Accident Tolerant Fuel, RCIC System, Station Blackout

1. INTRODUCTION

The Fukushima Daiichi accidents provided both insights into BWR operation under severe accident conditions and strong motivation for reactor safety enhancements. Unexpectedly, the Fukushima Daiichi Unit 2 and Unit 3 RCIC Systems successfully provided passive decay heat removal well beyond their expected operation time. Additionally, since the Fukushima Daiichi accidents, the nuclear power industry and its stakeholders have shown significant interest in advanced fuel systems, namely ATF, that can better withstand severe accident conditions. If coupled, the RCIC System and ATF could provide simple and inexpensive strategies for enhancing BWR safety using existing equipment and advanced near-term fuel designs.

The motivation for this project stems from the potential to increase the ability of existing nuclear power plants to passively respond to beyond design basis events (BDBE) using existing equipment and without changes to the plants. ATF lead assemblies, including one full ATF assembly, were introduced into reactor cores in 2019 for the purpose of improved fuel performance. However, ATF has several features that may also provide greater thermal margin and thereby enhance reactor safety. Similarly, the capabilities of the RCIC System might not be fully utilized for providing cooling water to the reactor core.

The authors are investigating the coupled use of ATF and the RCIC System to enhance safety of BWRs under BDBE conditions. ATF will generate most of the heat that needs to be removed from inside the Reactor Pressure Vessel and the RCIC System removes this heat, condenses the steam and returns water back to the Reactor Pressure Vessel. This simplistic version of an energy balance suggests that using ATF and the RCIC System in a combined way can enhance reactor safety to a significant extent. If successful, this project will result in simple and

[1] Contact author: cfaucet@sandia.gov

Sandia National Laboratories is a multimission laboratory managed and operated by National Technology & Engineering Solutions of Sandia, LLC, a wholly owned subsidiary of Honeywell International Inc., for the U.S. Department of Energy's National Nuclear Security Administration under contract DE-NA0003525.

inexpensive strategies to use existing equipment and fuel designs for enhanced Boiling Water Reactor Safety

This work used the MELCOR severe accident analysis code [1] [2]. MELCOR is a fully integrated severe accident analysis code developed by Sandia National Laboratories (SNL) for the NRC. MELCOR modeling capabilities include the thermal-hydraulic response, core heat-up and degradation, material relocation, core-concrete attack, hydrogen production and combustion, and fission product release/transport behavior during reactor accidents. This wide range of severe accident phenomena captured made MELCOR an appropriate tool for this work.

This paper is presented in five sections. First, a background overview of ATF is presented including its associated models in MELCOR. Then, the BWR model, accident scenario, and evaluation metrics are described. The next section presents simulations results and key findings. Finally, the concluding section gives a summary of insights gained and areas for future work.

2. BACKGROUND

As previously discussed, the Fukushima Daiichi accidents provided an industry catalyst for the development of advanced fuel system designs that improve reactor performance during both expected and unexpected reactor conditions. An objective of such systems is larger safety margins and increased coping time during a severe accident.

One ATF concept that achieves the aforementioned goals involves replacing traditional fuel pin Zircaloy cladding with FeCrAl alloys. FeCrAl has traditionally been used in industrial applications which require oxidation resistance in high temperature conditions [3] [4]. Accordingly, with respect to reactor operation, the primary benefit of FeCrAl is reduced oxidation in high temperature, steam-rich environments. During a severe accident, high temperature Zircaloy reactions with steam produce a runaway oxidation reaction that releases significant amounts of energy and combustible H_2 gas. Although the aluminum in FeCrAl will also oxidize with steam, its oxidation reaction produces roughly half of the energy of the Zircaloy oxidation reaction.

In response to needs for non-traditional reactor design modeling capabilities, SNL merged a FeCrAl model developed by Idaho National Laboratory with the main MELCOR code trunk. Before the FeCrAl model, MELCOR required mechanistic input to approximate non-Zircaloy oxidation kinetics and material properties. In contrast, the new FeCrAl model uses experimental-based correlations to accurately model FeCrAl response under reactor accident conditions. The following subsection provides a general description of the FeCrAl model.

2.1. MELCOR FeCrAl Model

To support the accident analyses of FeCrAl cladding employed by ATF, the default clad material permissible for reactor applications was recently extended in MELCOR 2.2 to include FeCrAl. The commercially available product provided by Kanthal, Kanthal-AMPT [5], was initially implemented to represent the material. Constant material properties and temperature dependent properties were taken from [5] and [3], respectively, to define the required material properties necessary for the MELCOR code. Application of Kanthal-AMPT also determined the mass fractions of the constituents as 74% Fe 21% Cr and 5% Al.

Oxidation is modeled within MELCOR based on the local material temperature, oxidant availability, and the oxidation regime, which is either pre- or post-breakaway (i.e. onset of cracks in cladding lattice structure). For steam environments, the regimes are based on experimental data which have demonstrated approximate temperatures signifying the initiation of breakaway oxidation; therefore, the temperature criterion are simple surrogates for the physio-chemical processes which alter the oxidation rate. A linear interpolation is applied from 1475 C to 1500 C, transitioning the oxidation rates from pre- to post-breakaway oxidation corresponding with observed onset of breakaway, as seen in [6].

Pre-breakaway oxidation rates are computed from available FeCrAl data; however, the post-breakaway is assumed to react the remaining material at rates similar to stainless-steel. The post-breakaway rate constants coefficients were not available at the time that FeCrAl material was added.

Pre- and post-breakaway oxidation rates in steam environments are given by the following expression for the mass of material, W:

$$\frac{dW^2}{dt} = K(T) \tag{1}$$

The rate constant value, $K(T)$, is determined experimentally [6] at constant temperatures and are represented by an Arrhenius equation:

$$K(T) = A\, e^{\frac{B}{T}} \tag{2}$$

Since the experimental data are gathered by weighing the samples, the multiplicative constant, A, is expressed in similar units (kg^2/m^4-s for mass gained). Within the MELCOR code, the rate constant is expressed as the mass of material reacted. This mass is simply converted from the fitted experimental data given assumed oxide forms from prescribed chemical equations of the material constituents and their mass fractions. The assumed reactions for Fe, Cr, and Al are presently limited to the following:

$$\mathrm{Fe} + \frac{4}{3}\mathrm{H_2O} \rightarrow \frac{1}{3}\mathrm{Fe_3O_4} + \frac{4}{3}\mathrm{H_2} + \mathrm{Q_{ox}} \tag{3}$$

$$\mathrm{Cr} + \frac{3}{2}\mathrm{H_2O} \rightarrow \frac{1}{2}\mathrm{Cr_2O_3} + \frac{3}{2}\mathrm{H_2} + \mathrm{Q_{ox}} \tag{4}$$

$$\mathrm{Al} + \frac{3}{2}\mathrm{H_2O} \rightarrow \frac{1}{2}\mathrm{Al_2O_3} + \frac{3}{2}\mathrm{H_2} + \mathrm{Q_{ox}} \tag{5}$$

The reaction energies, Q_{ox}, from the chemical equations are not specific to the assumed chemical reactions. Instead, the values applied for the general oxidation energies defined for Fe and Cr are taken from the existing oxidation model for stainless-steel. Similarly, the aluminum oxidation reaction energy is taken

from an existing aluminum oxidation model available within MELCOR. Fe, Cr, and Al reaction energies are -2.495x10^5 J/kg$_{Fe}$, 2.442x10^6 J/kg$_{Cr}$, and 1.518x10^7 J/kg$_{Al}$.

Figure 1 shows a comparison between the oxidation rates between zirconium, stainless-steel and FeCrAl for general comparison given the above assumptions. The rate constant multiplicative and exponential constants, A and B, are 4360 (kg^2/m^4-s) and -41376 (K), respectively, for the pre-breakaway oxidation for FeCrAl, the remaining coefficients for zirconium and stainless-steel are documented within the MELCOR reference material [1] [2].

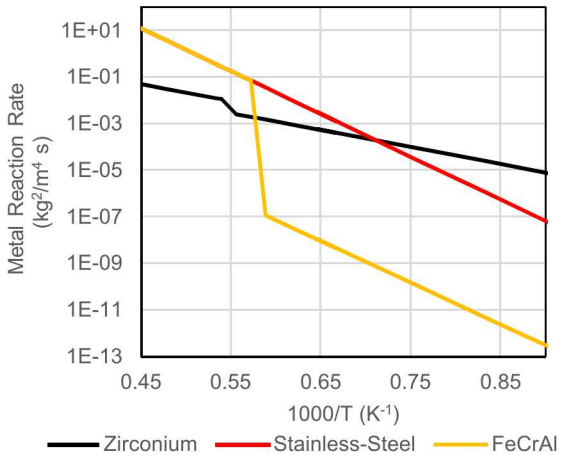

Figure 1: MELCOR OXIDATION RATE KINETICS CONSTANTS

2.2. MELCOR RCIC System Mechanistic Models

For mechanistic modeling of the RCIC system in MELCOR, a homologous pump model, a Terry turbine model (to include pressure and velocity stage models), and a rigid shaft model were added to the code [2].

A homologous pump model was integrated into MELCOR to predict the attending fluid momentum source (pressure head) of a centrifugal pump as a function of impeller speed and capacity (or volumetric flow). The model also computes hydraulic torque, pump friction torque, pump inertia, and pump energy dissipation

The Terry turbine is an integral part of BWR RCIC systems and can be mathematically represented as a combination of a pressure stage and one or more velocity stages. Terry turbine models were added to MELCOR to predict steam expansion in the pressure stage (to include two-phase steam supersaturation effects) and to calculate the momentum flux delivered to the turbine rotor by steam and/or water jets after expansion in nozzles. The pressure stage model predicts steam expansion as an assumed sequence of idealized processes (e.g. isentropic flow and Rayleigh flow with an analytical Wilson point model). The velocity stage model utilizes an angular momentum balance to predict shaft torque due to fluid action on the Terry turbine rotor.

A rigid shaft model was added to MELCOR in order to tie together both aforementioned turbomachinery models. In the RCIC system, the Terry turbine is coupled to a centrifugal pump via a rigid torque shaft such that there is a single, synchronous shaft speed dictated by an overall torque balance. The rigid shaft model computes shaft speed (i.e. turbine rotor speed which equals pump impeller speed) from a torque-inertia equation. The Terry turbine model furnishes a turbine torque, the homologous pump model furnishes an opposing impeller torque, and other sub-models calculate moments-of-inertia, friction torques, and miscellaneous user-defined torque terms.

3. ANALYSIS METHODOLOGY

The analysis methodology for this work was straightforward. A generic boiling water reactor MELCOR input was developed. Options for FeCrAl and Zircaloy cladding were added, and LTSBO scenarios were simulated for each cladding type. Timing and core damage metrics were used to compare the response of each cladding type.

With guidance from Sandia generic boiling water reactor MELCOR model was developed. The basis for the model was a Fukushima Unit 3 MELCOR input released by VTT Technical Research Centre of Finland (VTT) as supplement to Fukushima work [7]. Using insights gained from the Peach Bottom Uncertainty Analysis (UA) combined with new RCIC System and ATF models, the original VTT model was enhanced to provide a state-of-the-art platform for boiling water reactor MELCOR simulations [8].

This section details each step of the analysis methodology. The first section gives a brief outline of the BWR model characteristics. The second section discusses enhancements made to the original VTT model. The third section describes the modeling of the RCIC system. Finally, the fourth section outlines the scenario used and all associated boundary conditions.

3.1. Boiling Water Reactor Model Description

Table 1 lists design parameters for the BWR model. The power, masses, and volumes were all preserved from the original model. The mass flow rates were determined using a steady-state initialization process (described below). The FeCrAl cladding mass was calculated by assuming identical cladding geometries and scaling the Zircaloy mass using the ratio of FeCrAl's to Zircaloy's densities (7.20 g/cm^3 to 6.56 g/cm^3).

Table 1: BWR MODEL DESIGN PARAMETERS

Parameter	Value
Core Power	2381.0 MW$_{th}$
UO_2 Mass	105500 kg
Cladding Mass (Zircaloy/FeCrAl)	49954 kg / 54828 kg

RPV Pressure (nominal)	7.2 MPa
Peak Fuel Temperature	830.5 K
Core Mass Flow Rate	9978.9 kg/s
Total Recirculation Mass Flow Rate	3128.8 kg/s
Total Steam Output	1179.1 kg/s
Drywell Free Volume	4047.0 m^3
Suppression Pool Volume	2958.9 m^3

The BWR model has a typical reactor pressure vessel layout, as shown in Figure 2. Figure 2 displays the reactor pressure vessel control volume nodalization with arrows representing flow directions during normal operation (i.e. prior to an initiating event). The four main steam lines, A-D, are not displayed.

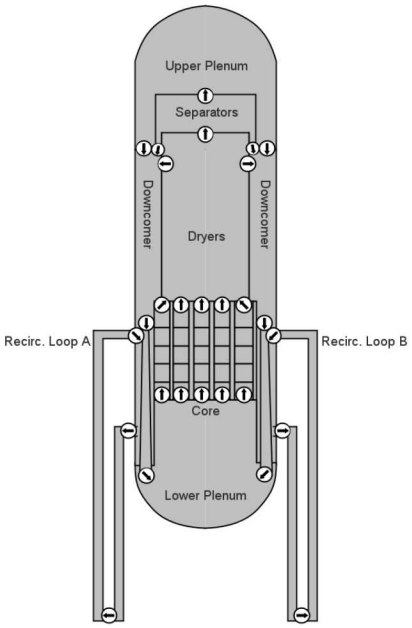

Figure 2: BWR MODEL RPV HYDRODYNAMIC NODALIZATION

Figure 3 shows the BWR model containment including the drywell, wetwell, and RCIC system. To simplify Figure 3, only main steam line B is shown, and the RCIC turbine and pump locations are significantly higher than their actual location in the model. The drywell is adiabatic, but the wetwell walls are thermally coupled by a heat structure to an environmental control volume representing the torus room. Since beyond design basis simulation was outside the scope of this work, the drywell does not contain a cavity for ex-vessel debris or leakage pathways (e.g. head flange lifting).

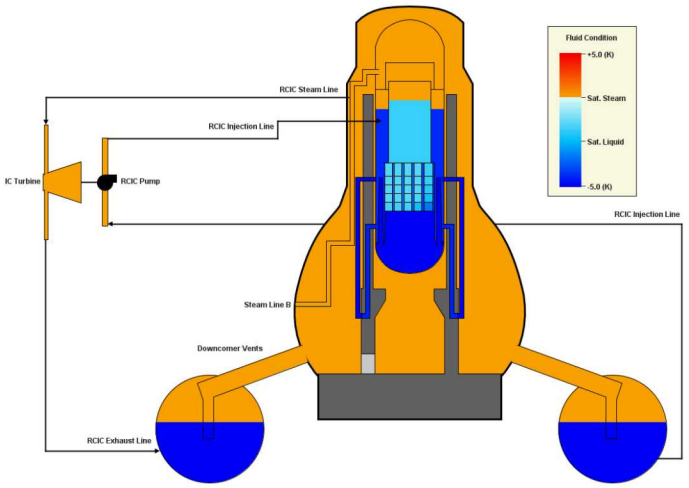

Figure 3: BWR MODEL CONTAINMENT AND RCIC SYSTEM

Each main steam line has two safety relief valves. The safety relief valve setpoints are staggered such that only one valve should cycle at any given time. The lowest setpoint safety relief valve opens at 7.54 MPa and recloses at 7.25 MPa. The remaining safety relief valve upper and lower setpoints increase incrementally by 0.2 MPa (i.e. 7.56/7.27 MPa, 7.58/7.29 MPa) to a maximum of 7.68 MPa and 7.38 MPa, respectively. The lowest setpoint safety relief valves are off of main steam line A.

The BWR model uses an internal MELCOR reference decay heat curve. The decay heat curve is based off a reference core inventory. Full documentation of the MELCOR reference core is available in the MELCOR documentation.

One assumption in MELCOR is that FeCrAl and Zircaloy have the same gap release criteria. Gap release occurs in MELCOR when the cladding temperature either reaches 1173 K or when cladding geometry is lost due to candling or oxidation. The cladding failure criteria was not modified for this work i.e. no special consideration was given to FeCrAl gap release.

3.2. Model Enhancements

A 500 s steady-state initialization was added to represent plant operation prior to an initiating event. Use of an initialization period prevents transients prior to the actual accident transient itself. During the steady-state period, a proportional-integral feedwater mass flow rate controller enforces two initial conditions – the downcomer level ### m above top of active fuel and equal mass flow into and out of the reactor pressure vessel. To control system pressure, a control volume representing the power conversion system held at 6.9 MPa was added downstream of the main steam lines. By the end of the initialization period, the model achieves the steady-state operating conditions listed in Table 1.

The reactor core nodalization was expanded to five rings, each with ten axial levels. In the Peach Bottom State-of-the-Art

Reactor Consequence Analysis Study (SOARCA), the ring areas and masses were divided in a way that preserved the radial power distribution from plant operating conditions [9]. The BWR model was assumed to have the same radial power distribution, and the existing core masses and flow areas were reapportioned accordingly. The core bypass area was also divided relative to the flow area of each ring.

The wetwell was also renodalized to reflect post-Fukushima insights that demonstrated earlier containment pressurization from localized suppression pool heating and vapor break-through. Figure 4 shows the radial and axial wetwell nodalization. Based on SNL recommendations, the wetwell was divided radially into 1/8th and 7/8th sections [10]. Both RCIC and the lowest setpoint SRV exhaust into the 1/8th section. The RCIC pump pulls from the 7/8th section. To model buoyancy-driven natural circulation, two flow paths connect the upper and lower portions of each radial volume where upper and lower refer to the flow area above and below the downcomer vent base elevation.

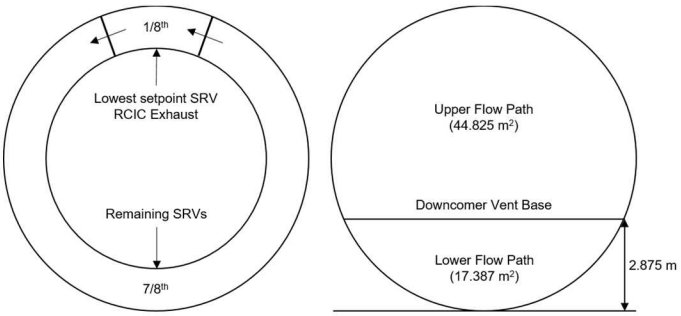

Figure 4: RADIAL AND AXIAL WETWELL HYDRODYNAMIC NODALIZATION

Safety relief valve thermal failure logic was added to simulate thermal deformation of the valve that could prevent it from reclosing. Whenever a valve is open, heat transfer to a heat structure representing the valve stem is enabled. No heat transfer to the valve stem occurs when the valve is closed. Once the representative heat structure reaches 900 K, the valve stem is assumed to deform in a way that does not allow the valve to reclose. This is modeled by forcing the safety relief valve to remain fully open.

3.3. RCIC Model

The existing RCIC model was upgraded to leverage recent MELCOR code developments. Specifically, a new RCIC systems-level model was developed that explicitly represents RCIC components (e.g. Terry turbine, turbo-shaft, nozzles). The new RCIC model provides an upgrade over previous mechanistic representations of the RCIC system. A full description of the RCIC model upgrades is available in Section 2.2.

Table 2 gives the RCIC design parameters. Because no vendor data was available, design parameters parameters from an SNL Fukushima Unit 2 study were used. The target injection rate was assumed from data provided in the Peach Bottom SOARCA report. The target downcomer level is 2.54 m (100 in.) below the main steam line nozzle to prevent turbine flooding. The RCIC pump input uses the internal MELCOR two-phase homologous pump curves.

Table 2: RCIC DESIGN PARAMETERS

Parameter	Value
Turbine Rotor Radius	0.3 m (0.98 ft.)
Nozzle Width	0.01 m (0.39 in.)
Turbine Moment of Inertia	10 kg-m^2 (237 lb-ft^2)
Rated RCIC Speed	4300 rpm
Rate Pump Head	7.52 MPa (1090 psi)
Rated Pump Torque	499 N-m (331 ft-lb)
Pump Injection Flow Area	0.068 m^2 (0.180 ft^2)
Target Injection Rate	38.7 kg/s (616 gpm)
Target Downcomer Level	13.11 m (43.01 ft.)

During operation, RCIC flow is automatically controlled by the governor valve. The governor valve control actions were represented by a PI controller that maintains the target injection rate by increasing or decreasing its open fraction. This allowed for a relatively constant injection rate regardless of steam line pressure. However, these control actions require DC power to operate. When DC power is exhausted, the governor valve fails fully open which severely increases the probability of an overspeed trip.

RCIC failure occurs when either overspeed trip or pump cavitation conditions are met. An overspeed trip occurs when the turbine speed exceeds 5625 rpm, and the RCIC pump is assumed to cavitate when the suppression pool temperature exceeds 373.0 K. Although manual reset of the RCIC trip/throttle valve after and overspeed trip (i.e. blackstart) is a commonly credited operator action in blackout procedures, RCIC blackstart is prohibitively challenging to model using MELCOR control logic and was not included in the model.

3.4. Scenario Description

For this work, the scenario considered was an unmitigated LTSBO. An LTSBO occurs when all offsite and onsite AC power (e.g. diesel generators) sources are lost. For a BWR, the only available emergency core cooling system is RCIC. Unmitigated refers to the lack of successful operator actions to restore power or connect FLEX equipment.

A seismic event similar to the Peach Bottom SOARCA was chosen as the initiating event. The seismic event is assumed to disable all sources of AC power, creating a LTSBO. FLEX equipment is either inaccessible or inoperable. However, RCIC and all associated components are accessible and operable. Station batteries supply DC power for 4 hours, their assumed

lifetime. Operators are available to perform level and pressure control actions described below.

Level control actions were credited based on station blackout procedures [11]. Following loss of power, operators actuate RCIC immediately when the downcomer water level begins to decrease. RCIC startup is assumed to take 60 s. Operators are assumed to maintain the downcomer level 2.54 m below the main steam line penetrations at 15.646 m using the RCIC steam supply valve. This action is performed until a RCIC failure condition is met.

Pressure control actions were also credited, again based on station blackout procedures [11]. All pressure control actions assumed use of the lowest setpoint SRV. In order, the referenced procedures specify that operators should:

- Maintain the reactor pressure below 1065 psig (7.444 MPa) until the suppression pool reaches 120 °F,
- Perform a controlled depressurization to 150 psig (1.136 MPa) at 50 °F/hr (7.716×10^{-3} K/s) when the suppression pool temperature reaches 120 °F (322 K), and
- Maintain the reactor pressure between 150 to 250 psig (1.136 to 1.825 MPa).

Because the procedures only provide an upper pressure limit for the first action, operators were assumed to cycle between 800 and 1000 psig (5.617 and 6.996 MPa). The controlled depressurization begins when the 7/8th wetwell volume suppression pool temperature reaches 150 °F (322 K).

The scenario ends when 100 kg of core material (e.g. cladding, fuel, support structures) debris forms. 100 kg is less than 0.1% of the total core mass, meaning that the scenario ends at the onset of significant core damage. Given the current gaps in the MELCOR FeCrAl model, this end condition also prevents non-physical results from coarse approximations of FeCrAl cladding degradation.

4. RESULTS AND INSIGHTS

A single simulation was performed for each cladding material type using the scenario described in Section 3.4. This section presents findings and compares results for each simulation. The first subsection gives a walkthrough the accident sequence for each simulation. The second subsection discusses findings and areas for future work.

Both simulations were performed using MELCOR 2.2.14819, an internal SNL build.

4.1. Accident Sequence

A set of severe accident event timings were selected based on their use in the Peach Bottom UA. The timing metrics were chosen based on their ability to characterize the accident sequence. Table 3 compares event timings for both simulations.

Table 3: EVENT TIMINGS FOR ZIRCALOY AND FECRAL SIMULATIONS

Event	Time (h)	
	Zircaloy	FeCrAl
Initiating Event	0.00	0.00
Reactor SCRAM	0.00	0.00
RCIC Actuation	0.02	0.02
Station Batteries Exhausted	4.00	4.00
RCIC Overspeed Trip	4.00	4.00
RPV Level at Top of Active Fuel	5.71	5.73
RPV Level Below Active Fuel	6.86	6.91
First H_2 Production	7.72	8.20
First Gap Release	8.24	8.22
SRV Thermal Failure	8.61	8.65
10kg of H_2 Produced	8.35	9.31
100kg of Debris Produced	9.60	9.94

Except for hydrogen production timings, both runs showed comparable results. Prior to station battery failure at 4.00 h, there is no difference in event timings. When the station batteries exhaust at 4.00 h, a RCIC overspeed trip occurs immediately in both runs. Beyond 4.00 h, the largest differences in timings occur with respect to hydrogen production. Oxidation occurs about 0.5 h earlier for the Zircaloy simulation, and it takes almost 1.0 h longer for the FeCrAl simulation to produce 10 kg of H_2. Despite these differences, both runs predict similar times for gap release and SRV thermal failure. The FeCrAl run ends 0.34 h later than the Zircaloy run which suggests a slower rate of core heatup and degradation.

Figure 5 and Figure 6 show the RPV level and pressure, respectively. In both figures, little difference is observed between either simulation. Initially, the RPV level decreases while the RCIC pump builds enough pressure head to begin injection. During this time, operators begin to cycle the lowest setpoint SRV between 800 to 100 psig (5.617 to 6.996 MPa) as described in Section 3.4. After RCIC injection begins, the RPV level begins to rise. A pressure transient occurs while the RPV level increases as saturated coolant in the core region subcools. Operators continue to cycle the lowest setpoint SRV until loss of DC power at 4.0 h. The continuous cycling of the SRV in conjunction with operator level control actions causes the RPV level to oscillate. Once the station batteries fail, operators lose manual control of the SRV, and the system pressure quickly rises to the lowest SRV setpoint until SRV thermal failure.

Additionally, RCIC injection is lost, and the RPV level steadily boils off until the end of each simulation.

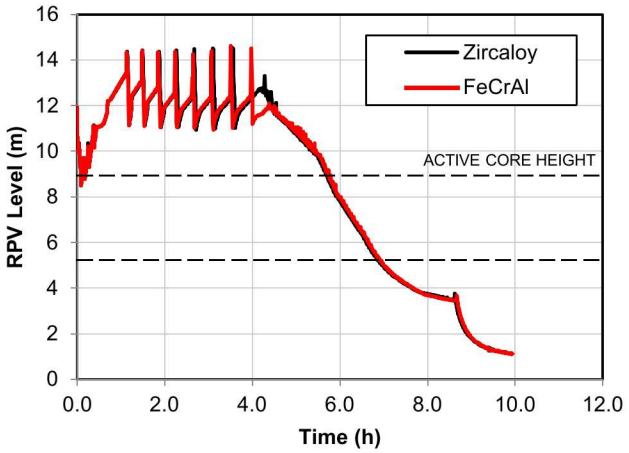

Figure 5: RPV PRESSURE FOR ZIRCALOY AND FECRAL SIMULATIONS WITH ACTIVE CORE HEIGHT NOTED

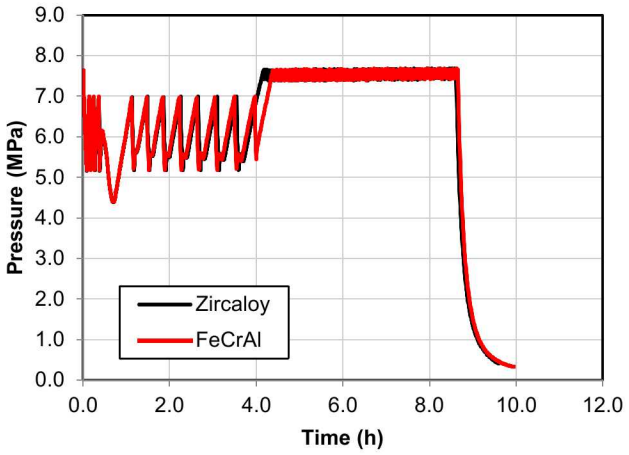

Figure 6: RPV PRESSURE FOR ZIRCALOY AND FECRAL SIMULATIONS

Figure 7 shows the peak cladding temperature for each simulation. Both simulations show nearly identical trends. After the initial drop in temperature at 0.0 h, the RCIC system provides sufficient cooling to maintain the cladding temperature just above 500 K. As the core slowly uncovers, the peak temperature begins to rise. At about 9.0 h, runaway oxidation occurs as energy released from oxidation reactions increases the rate of oxidation in a positive feedback loop. However, the reduced amount of energy produced by FeCrAl oxidation results in a slow rate of temperature increase for the FeCrAl run.

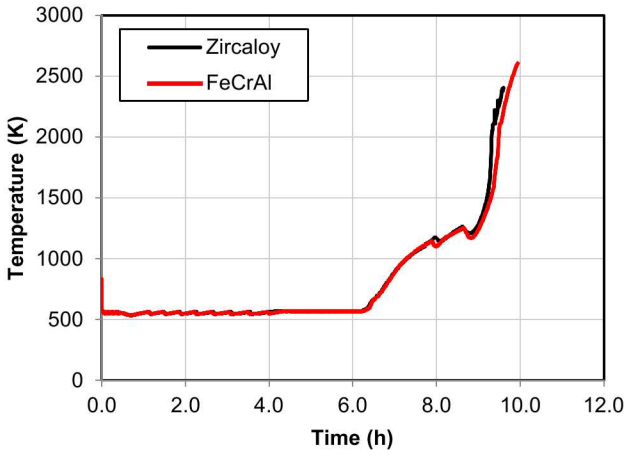

Figure 7: PEAK CLADDING TEMPERATURE FOR ZIRCALOY AND FECRAL SIMULATIONS

Figure 8 displays the total hydrogen mass produced during each simulation. The dashed line in Fig. Figure ***8*** denotes 10 kg. In total, the Zircaloy simulation estimated 266.11 kg of hydrogen production, whereas the FeCrAl simulation estimated 157.82 kg of hydrogen production. As expected, the FeCrAl run produces significantly less hydrogen, and its production occurs at a relatively slow rate compared to Zircaloy. Even during runaway oxidation at similar temperatures, FeCrAl produces less hydrogen at a slower rate than Zircaloy.

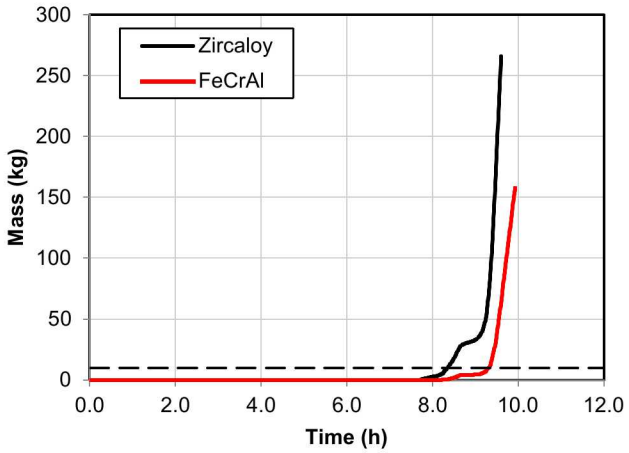

Figure 8: TOTAL HYDROGEN MASS PRODUCED FOR ZIRCALOY AND FECRAL SIMULATIONS WITH 10 KG NOTED

4.2. Discussion and Future Work

Besides hydrogen production, little difference was observed between the Zircaloy and FeCrAl simulations. Both accident sequences progressed similarly with little variation in RPV level, pressure, or peak fuel temperature. Ultimately, only a 0.34 h time

difference before the onset of core degradation was realized using FeCrAl in place of Zircaloy.

However, significant benefits were observed with respect to hydrogen production. Use of FeCrAl resulted in over 100 kg less hydrogen compared to Zircaloy and a reduced rate of runaway oxidation. The reduction in oxidation energy also produced a slightly more gradual temperature rise prior to fuel failure.

One area for improvement of this work is the use of a single boundary conditions, specifically the nuclide inventory and station battery availability. The Peach Bottom UA showed that the total decay heat and station battery availability had significant influence on the accident progression. Intuitively, higher amounts of decay heat result in a faster accident progression whereas longer battery availability slow the accident progression. While this work shows some increased coping time from FeCrAl, a full investigating into a range of scenario conditions could reveal further insights.

As noted by ORNL, empirical correlations for FeCrAl properties (e.g. specific heat, thermal conductivity) have some uncertainty [3]. MELCOR has the capability for users to modify material properties [1]. An area for future work would also be to study the effects of FeCrAl property uncertainty with respect to the metrics presented herein.

5. CONCLUSION

By combining state-of-the-art MELCOR modeling practices with new, physics-based RCIC System and ATF MELCOR inputs, the new BWR model presented herein provides a contemporary platform for BWR severe accident simulations. A study was performed to compare Zircaloy and FeCrAl ATF performance under BWR LTSBO conditions with RCIC operation using the MELCOR code. A state-of-the-art MELCOR BWR model was developed that utilized new RCIC and ATF models. Compared to Zircaloy, FeCrAl demonstrated a slower core degradation timeline with significantly less hydrogen production. Although the results are limited in scope, the presented analysis could easily be expanded to a full-scale uncertainty study that considers a range of severe accident boundary conditions.

ACKNOWLEDGEMENTS

The authors would like to thank Tuomo Sevón of VTT Technical Research Centre of Finland for making his Fukushima Unit 3 model publicly available.

The authors gratefully acknowledge financial support of this project by the US Department of Energy Consolidated Innovative Nuclear Research Project, Award No. DE-NE0008763.

Sandia National Laboratories is a multimission laboratory managed and operated by National Technology & Engineering Solutions of Sandia, LLC, a wholly owned subsidiary of Honeywell International Inc., for the U.S. Department of Energy's National Nuclear Security Administration under contract DE-NA000352

REFERENCES

[1] Humphries, L. L., Beeny, B. A., Gelbard, F., Louie, D.L., and Phillips, J., 2017, "MELCOR Computer Code Manuals, Vol. 1: Primer and Users' Guide, Version 2.2.9541," SAND2018-13559 O, Sandia National Laboratories, Albuquerque, NM.

[2] Humphries, L. L., Beeny, B. A., Gelbard, F., Louie, D.L., and Phillips, J., 2017, "MELCOR Computer Code Manuals, Vol. 1: Primer and Users' Guide, Version 2.2.9541," SAND2018-13560 O, Sandia National Laboratories, Albuquerque, NM.

[3] Field, K.G., Snead, M.A., Yamamoto, Y., and Terrani, K.A., 2017, "Handbook on the Material Properties of FeCrAl Alloys for Nuclear Power Production Applications," Oak Ridge National Laboratory, Oak Ridge, TN.

[4] Pint, B. A., Terrani, K.A., Brady, M.P., Cheng, T., and Keiser, J.R., 2013, "High Temperature Oxidation of Fuel Cladding Candidate Materials in Steam-Hydrogen Environments," Journal of Nuclear Materials 440(1-3), 420-427.

[5] Kanthal®, 2018, "Kanthal® APM Tube," from https://www.kanthal.com/en/products/material-datasheets/tube/kanthal-apm/.

[6] Robb, K.R., Howell, H., and Ott, L.J., 2018, "Design and Analysis of Oxidation Tests to Inform FeCrAl ATF Severe Accident Models," Oak Ridge National Laboratory, Oak Ridge, TN.

[7] Sevón, T., 2015, "A MELCOR model of Fukushima Daiichi Unit 3 accident," Nuclear Engineering and Design 284, 80-90.

[8] United States Nuclear Regulatory Commission, 2012, "State-of-the-Art Reactor Consequence Analyses Project: Uncertainity Analysis of the Unmitigated Long-Term Station Blackout of the Peach Bottom Atomic Power Station (Draft)," NUREG/CR-7115, United States Nuclear Regulatory Commission, Rockville, MD.

[9] United States Nuclear Regulatory Commission, 2013, "State-of-the-Art Reactor Consequence Analyses Project Volume 1: Peach Bottom Integrated Analysis," NUREG/CR-7110, United States Nuclear Regulatory Commission, Rockville, MD.

[10] Phillips, J., 2014, "Wetwell Modeling Nodalization Study and SNAP Post Processing".

[11] "Loss of AC Power Rev. 26b.", 2018.

[12] Electric Power Research Institute, 2019, "Accident-Tolerant Fuel Valuation: Safety and Economic Benefits (Revision 1)," Palo Alto, CA..

[13] Ross, K., Cardoni, J., Wilson, C., Morrow, C., Osborn, D., and Gauntt, R., 2015' "Modeling of the Reactor Core Isolation Cooling Response to Beyond Design Basis

Operations - Phase 1", SAND2015-10662, Sandia National Laboratories, Albuquerque, NM.